
MISAPP: MULTI-HOP INTENT-AWARE SESSION GRAPH LEARNING FOR NEXT APP PREDICTION

Yunchi Yang*
School of Mathematics
Shandong University,
Jinan 250100
ycyang@mail.sdu.edu.cn

Longlong Li*
School of Physical and Mathematical Sciences
Nanyang Technological University,
Singapore 637371
longlong.li@ntu.edu.sg

Jianliang Wu
School of Mathematics
Shandong University,
Jinan 250100
jlwu@sdu.edu.cn

Cunquan Qu[†]
Data Science Institute
Shandong University,
Jinan 250100
cqqu@sdu.edu.cn

ABSTRACT

Predicting the next mobile app a user will launch is essential for proactive mobile services. Yet accurate prediction remains challenging in real-world settings, where user intent can shift rapidly within short sessions and user-specific historical profiles are often sparse or unavailable, especially under cold-start conditions. Existing approaches mainly model app usage as sequential behavior or local session transitions, limiting their ability to capture higher-order structural dependencies and evolving session intent. To address this issue, we propose MISApp, a profile-free framework for next app prediction based on multi-hop session graph learning. MISApp constructs multi-hop session graphs to capture transition dependencies at different structural ranges, learns session representations through lightweight graph propagation, incorporates temporal and spatial context to characterize session conditions, and captures intent evolution from recent interactions. Experiments on two real-world app usage datasets show that MISApp consistently outperforms competitive baselines under both standard and cold-start settings, while maintaining a favorable balance between predictive accuracy and practical efficiency. Further analyses show that the learned hop-level attention weights align well with structural relevance, offering interpretable evidence for the effectiveness of the proposed multi-hop modeling strategy.

Keywords Next app prediction · Cold-start prediction · Graph neural networks · Dynamic intent modeling

1 Introduction

With the widespread adoption of smartphones, mobile applications have become an integral part of daily digital life [1]. Modern app ecosystems span diverse categories [2, 3, 4, 5], including social media, online shopping, navigation, short-video platforms, and productivity tools, enabling users to conveniently access digital services in a wide range of scenarios [6, 5]. In this context, accurately predicting the next app a user is likely to launch is important for proactive mobile services, as it can improve app recommendation quality, optimize device-level resource allocation [7, 8], enhance system responsiveness [9, 10], and facilitate network-level scheduling. Consequently, next app prediction has become an important problem in mobile user behavior modeling with both practical and research significance [11, 12, 13].

Despite its importance, accurate next app prediction remains challenging in real-world settings [14]. First, user intent may change rapidly within short sessions, and such changes are often context-dependent rather than strictly sequential.

*These authors contributed equally.

[†]Corresponding author.

As a result, models that mainly rely on fixed-order dependencies, such as RNN-based approaches [15] and Transformer-based sequence models [16, 17], may not fully capture fine-grained intent evolution from limited interactions. This challenge becomes more pronounced in cold-start scenarios, where user-specific histories are sparse or unavailable and intent must be inferred directly from current session behaviors.

Second, session-level app usage contains not only immediate transitions between consecutive apps but also higher-order structural dependencies that reflect latent behavioral routines and semantically related app usages [18, 19, 20]. Existing methods that mainly focus on raw sequences or 1-Hop session graph provide only a limited view of session structure, which may overlook long-range dependencies and cross-app latent relations.

Third, session-level app usage is also shaped by contextual conditions such as time and location [21, 22]. These cues can modulate the meaning of transition patterns and provide useful evidence for intent inference [23, 24]. However, many existing methods incorporate contextual information only weakly or independently from session structure, limiting their ability to jointly reason over behavioral dependencies and session conditions.

To address these challenges, we propose MISApp, a profile-free framework that infers next-app intent directly from session-level behaviors without assuming the availability of static user profiles. MISApp captures multi-range transition dependencies through multi-hop session graphs, models intent evolution from recent interactions, and incorporates temporal and spatial context to characterize session conditions. By combining structural dependency modeling with session-level intent inference, MISApp supports robust and accurate next app prediction, particularly in cold-start scenarios where personalized historical information is limited.

The contributions of our work are summarized as follows:

- **Multi-Hop Session Graph Modeling:** We propose a multi-hop session graph framework that explicitly decomposes app transitions into multiple structural ranges. By modeling both direct and higher-order dependencies within sessions, MISApp captures richer behavioral structure than conventional sequential or 1-Hop graph representations [25].
- **Profile-Free Intent Modeling for Cold-Start Prediction:** We develop a profile-free intent modeling framework that infers evolving user intent directly from recent session behaviors, without relying on static user profiles or long-term historical attributes. This design improves robustness in cold-start scenarios and better reflects short-term intent dynamics.
- **Empirical Validation and Structural Interpretability:** Extensive experiments on two real-world datasets show that MISApp outperforms competitive baselines under both standard and cold-start settings, while maintaining favorable practical efficiency. Additional analyses indicate that the learned hop-level attention aligns well with structural relevance, supporting the structural interpretability of the proposed multi-hop modeling mechanism.

2 RELATED WORK

Modeling mobile user behavior for the next app prediction fundamentally requires capturing structural dependency patterns within sessions, where different transition ranges may encode distinct semantic roles. This section reviews three research domains most relevant to our work: mobile app usage prediction, graph neural networks, and Transformer-based time-series predictors.

Mobile App Usage Prediction: Mobile app usage prediction aims to infer the next app a user is most likely to launch based on their historical behaviors and contextual cues. Prior studies typically cast this task as a time-series prediction problem, emphasizing dependencies across consecutive app launches. Classical models such as MRU and MFU [21] offer simple baselines but overlook temporal and contextual dependencies. To better capture sequential dynamics, deep learning-based models such as DeepApp [26], DeepPattern [27], NeuSA [23], MAPLE [28], and AppUsage2Vec [18] aim to encode app usage patterns together with contextual features. However, they struggle to distinguish higher-order behavioral routines, limiting their ability to adapt to rapid inter-session intent shifts.

Graph Neural Networks: Graph Neural Networks (GNNs) offer a powerful framework for modeling relational structures by propagating information across neighboring nodes [29, 30, 31], and thus have been widely adopted in sequential prediction and app recommendation. Graph-based models—such as SA-GCN [32], DUGN [33], and various Hypergraph-based approaches [34, 35]—capture structural dependencies within sessions and effectively model local interaction patterns among apps. However, such designs implicitly entangle structural ranges, as higher-order signals are mixed through repeated propagation rather than explicitly separated. Consequently, their interpretability remains somewhat limited due to the opaque mixing of structural ranges.

Transformer-based Time-Series Predictors: The Transformer [16] architecture, built upon self-attention, has demonstrated remarkable effectiveness in capturing long-range dependencies in sequential data. Although recent time-series forecasting architectures such as Reformer [36], FEDformer [37], and TimesNet [38]—achieve high performance in general time-series forecasting tasks, they are not tailored for user behavior modeling and overlook essential contextual signals such as temporal and spatial factors, which are critical for personalized app prediction. Appformer [24] integrates multi-modal progressive fusion and sophisticated feature extractors. However, its focus on long-range sequential dependencies limits its ability to capture rapid intention shifts within user-app interactions..

3 METHODOLOGY

Problem Definition: Let $\mathcal{A} = \{a_1, a_2, \dots, a_{|\mathcal{A}|}\}$ denote the set of all mobile applications, and let $\mathcal{R} = \{r_1, r_2, \dots, r_{|\mathcal{R}|}\}$ denote the set of all base station IDs. For each user, the raw behavior log is a time-ordered sequence of app usage events

$$\mathcal{X} = ((a_1, t_1, r_1), (a_2, t_2, r_2), \dots, (a_N, t_N, r_N)), \quad (1)$$

where $a_i \in \mathcal{A}$ is the app launched at the i -th event, t_i is its timestamp, and $r_i \in \mathcal{R}$ is the corresponding base station ID.

We segment the event sequence into sessions according to an inactivity threshold δ_t : two consecutive events are assigned to the same session if and only if

$$t_{i+1} - t_i \leq \delta_t. \quad (2)$$

In our experiments, $\delta_t = 300$ seconds.

After segmentation, each session S is represented as an ordered sequence of app usage events:

$$S = (s_1, s_2, \dots, s_T), \quad s_i = (a_i, t_i, r_i), \quad (3)$$

where T denotes the session window size. Let $\tau \in \{0, 1, \dots, 23\}$ denote the hour-of-day of the last event in the session, and let $\rho \in \mathcal{R}$ denote the base station ID of the last event in the session.

Given the current session S together with its temporal context τ and spatial context ρ , the task is to predict the next app $a_{T+1} \in \mathcal{A}$. Formally, the model estimates

$$P(a_{T+1} | S, \tau, \rho), \quad (4)$$

and outputs the most likely app as the prediction

$$\hat{a}_{T+1} = \arg \max_{a \in \mathcal{A}} P(a | S, \tau, \rho). \quad (5)$$

3.1 Framework Overview

We propose MISApp, an intent-aware app prediction framework built on multi-hop session graphs. As illustrated in Figure 1A, the architecture comprises four key components:

- **Multi-Hop Relation Graph Module:** MISApp constructs 1-Hop, 2-Hop, and 3-Hop session graphs based on temporal relations between apps. LightGCN is applied to each graph to learn structural representations.
- **Contextual Information Embedding:** Session temporal context and spatial context (derived from clustered base station IDs) are embedded into a unified vector space, providing complementary signals for modeling user behavior.
- **Cross-Modal Gated Fusion:** MISApp employs a cross-modal gated fusion mechanism that uses a learnable sigmoid gate to adaptively balance the contributions of intent-aware features from different modalities.
- **Inter-Session Intent Transition Module:** To capture evolving user interests, MISApp extracts the most recent apps as an immediate intent signal and leverages a Transformer to model dynamic intent by fusing this signal with session-level structural embeddings.

3.2 Multi-Hop Relation Graph Module

App Embedding Layer: Each app $a \in \mathcal{A}$ is associated with a learnable embedding vector $e_A(a) \in \mathbb{R}^d$, where d is the embedding dimension.

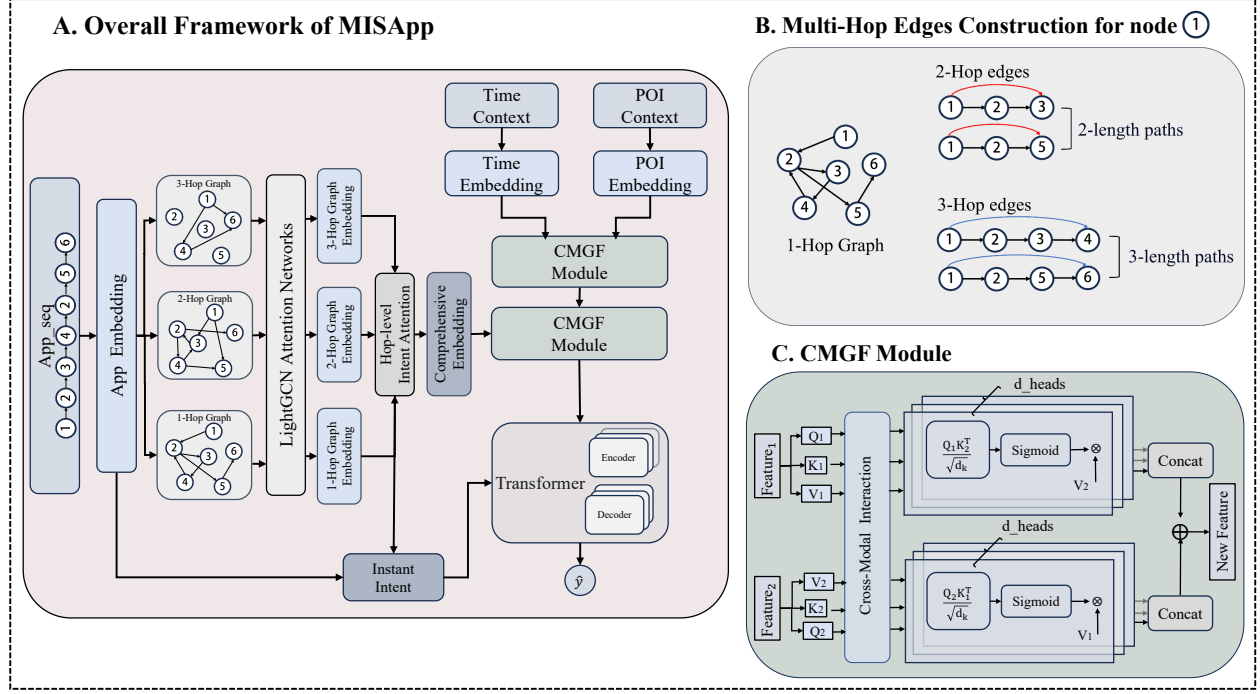


Figure 1: The overall framework of MISApp: the model integrates app, temporal and spatial context embedding through cross-modal gated fusion (CMGF) module, constructs multi-hop session graph, and obtains multi-hop structural features through lightgcn attention network. The generated graph embedding is combined with the immediate intent and processed by the transformer layer, which captures the sequential dependencies necessary for predicting the next app.

Session Graph Construction: The sequential usage behavior of user applications can be effectively modeled as a graph structure to capture the underlying transition patterns within a session. Given a user’s historical app interaction sequence in session S , we construct a directed session graph:

$$G_1^S = (V^S, E_1^S), \quad (6)$$

where

$$\begin{aligned} V^S &= \{a_t \mid 1 \leq t \leq T\} \subseteq \mathcal{A}, \\ E_1^S &= \{(a_t, a_{t+1}) \mid 1 \leq t < T\}. \end{aligned} \quad (7)$$

Each directed edge in E_1^S represents an immediate transition between two consecutive app events.

By representing the session as a directed graph, the model can go beyond raw linear sequences to reflect the intrinsic transition structure of user actions. This 1-Hop session graph G_1^S serves as the fundamental structural representation, providing a basis for capturing more complex, higher-order dependencies in subsequent modules.

Although the 1-Hop session graph structure can effectively capture direct adjacency relations within each session, it cannot model longer-range behavioral dependencies. In session-based app usage, different hop distances encode distinct semantic roles: immediate transitions reflect short-term intent continuity, while higher-order connections capture latent procedural routines. To capture such latent structures, we extend the graph representation to include multi-hop connectivity, as illustrated in Figure 1B.

E_1^S denotes the set of directed edges in the original 1-Hop session graph. We construct higher-hop connections by composing edges along reachable paths while excluding self-loops. Specifically, the 2-Hop edge set is defined as

$$\begin{aligned} E_2^S &= \{(a_u, a_w) \mid a_u \neq a_w, \exists a_v \text{ s.t.} \\ &\quad (a_u, a_v) \in E_1^S, (a_v, a_w) \in E_1^S\}. \end{aligned} \quad (8)$$

Similarly, the 3-Hop edge set is obtained by extending the composition to three consecutive edges:

$$E_3^S = \{(a_u, a_x) \mid a_u \neq a_x, \exists a_w \text{ s.t.} \\ (a_u, a_w) \in E_2^S, (a_w, a_x) \in E_1^S\}. \quad (9)$$

Accordingly, the γ -Hop session graph is defined as

$$G_\gamma^S = (V^S, E_\gamma^S), \quad \gamma \in \{1, 2, 3\}. \quad (10)$$

The 1-Hop session graph captures immediate transition continuity, whereas the 2-Hop and 3-Hop session graphs encode longer-range behavioral dependencies. **LightGCN Attention Networks:** To encode the multi-hop session graphs efficiently, we adopt a LightGCN-based propagation mechanism [39]. Compared with conventional graph convolution schemes that combine neighborhood aggregation with feature transformation and nonlinear activation, LightGCN retains a lightweight propagation rule centered on neighbor aggregation. This makes it well suited to our setting, where the goal is to capture structural dependencies over session graphs while keeping the encoder simple and computationally efficient.

To capture structural dependencies at different ranges, we construct three session graphs—1-Hop, 2-Hop, and 3-Hop—and perform LightGCN-based propagation on each graph separately. For the γ -th graph $G_\gamma^S = (V^S, E_\gamma^S)$, the adjacency relations encode direct transitions, two-step dependencies, and longer-range three-step dependencies, respectively. By applying propagation independently on each graph, MISApp preserves structural information at different hop ranges rather than mixing them within a single propagation process. For the γ -th graph G_γ^S , the layer-wise propagation is defined as

$$n_v^{(l+1, \gamma)} = \sum_{u \in \mathcal{N}^{(\gamma)}(v)} \frac{1}{\sqrt{|\mathcal{N}^{(\gamma)}(v)|} \sqrt{|\mathcal{N}^{(\gamma)}(u)|}} n_u^{(l, \gamma)}, \quad (11)$$

where $n_v^{(0, \gamma)} = \mathbf{e}_A(v)$ denotes the initial app embedding in graph G_γ^S , obtained from the App Embedding Layer. l indexes the propagation layer and $\mathcal{N}^{(\gamma)}(v)$ denotes the set of neighbors of node v in G_γ^S . After L_g layers, node representations are obtained by layer-wise averaging:

$$n_v^{(\gamma)} = \frac{1}{L_g + 1} \sum_{l=0}^{L_g} n_v^{(l, \gamma)}. \quad (12)$$

To obtain a graph-level embedding for G_γ^S , we apply an attention mechanism that highlights the apps most relevant to the user’s immediate intent. For each v in G_γ^S , the attention coefficient is computed as

$$\alpha_v^{(\gamma)} = \frac{\mathcal{S}(\mathbf{W}_Q n_{a_T}^{(\gamma)}, \mathbf{W}_K n_v^{(\gamma)})}{\sum_{u \in V^S} \mathcal{S}(\mathbf{W}_Q n_{a_T}^{(\gamma)}, \mathbf{W}_K n_u^{(\gamma)})}, \quad (13)$$

where $\mathcal{S}(\cdot)$ is Scaled Dot-Product Attention and $\mathbf{W}_Q, \mathbf{W}_K, \mathbf{W}_V$ are learnable projection matrices. The graph-level embedding is obtained by

$$\mathbf{g}^{(\gamma)} = \sum_{v \in V^S} \alpha_v^{(\gamma)} \mathbf{W}_V n_v^{(\gamma)}. \quad (14)$$

Let the immediate intent window size be K . The last K applications in the current session are denoted as $\{a_{T-K+1}, \dots, a_T\}$, and their corresponding semantic application embeddings are $\{n_{a_{T-K+1}}^1, \dots, n_{a_T}^1\}$. The short-term immediate intent of the current session is represented as:

$$\mathbf{s} = \mathbf{W}[n_{a_{T-K+1}}^1, \dots, n_{a_T}^1], \quad (15)$$

where $\mathbf{W} \in \mathbb{R}^{d \times Kd}$ are learnable parameters.

To adaptively integrate the information from different graph scales, we propose the Hop-level Intent Attention mechanism. We treat each hop representations as structural memory candidates and utilize the short-term immediate intent \mathbf{s} as a query to dynamically determine the importance of each hop, ensuring that the final session representation is precisely aligned with the user’s current interaction context. The attention weight W_{hop_γ} for the embedding of the γ -Hop session graph $\mathbf{g}^{(\gamma)}$ with respect to the intent vector \mathbf{s} is defined as:

$$W_{hop_\gamma} = \frac{\exp(\mathbf{s}^\top \cdot \mathbf{g}^{(\gamma)})}{\sum_{\gamma=1}^3 \exp(\mathbf{s}^\top \cdot \mathbf{g}^{(\gamma)})}, \quad (16)$$

then the comprehensive embedding \mathbf{g} is constructed as a weighted sum of the multi-hop session graph embeddings:

$$\mathbf{g} = \sum_{\gamma=1}^3 W_{hop_\gamma} \mathbf{g}^{(\gamma)} \in \mathbb{R}^d. \quad (17)$$

3.3 Contextual Information Embedding

To enhance the expressiveness of session representations, our work incorporates two types of contextual signals: temporal context [40] and spatial context [41]. These contextual embeddings provide complementary information that helps characterize how users interact with mobile applications under different temporal patterns and environmental settings.

Temporal Context Embedding: To incorporate temporal context into the user behavior model, the hour-of-day $\tau \in \{0, 1, \dots, 23\}$ of the last app event in app usage session S is associated with a learnable embedding

$$\mathbf{e}_T^{(\tau)} = \mathbf{E}_T[\tau, :], \quad (18)$$

where $\mathbf{E}_T \in \mathbb{R}^{24 \times d}$ is a trainable temporal embedding matrix and $\mathbf{e}_T^{(\tau)} \in \mathbb{R}^d$ denotes the embedding of hour τ .

Spatial Context Construction and Embedding:

Spatial Context Construction Each base station ID in Tsinghua App Usage is associated with a set of POI (Point-of-Interest) environmental attributes, such as the number of nearby pharmacies, hotels, stadiums, and other facilities. We represent each base station $r \in \mathcal{R}$ is associated with a POI feature vector

$$\mathbf{x}_r = (x_{r,1}, x_{r,2}, \dots, x_{r,M}) \in \mathbb{R}^M, \quad (19)$$

where M denotes the number of POI feature dimensions.

We first perform feature-wise min-max normalization:

$$\tilde{x}_{r,m} = \frac{x_{r,m} - \min_{q \in \mathcal{R}} x_{q,m}}{\max_{q \in \mathcal{R}} x_{q,m} - \min_{q \in \mathcal{R}} x_{q,m}}, \quad m = 1, 2, \dots, M. \quad (20)$$

Let $\tilde{\mathbf{x}}_r \in \mathbb{R}^M$ denote the normalized POI vector of base station r . We then define the contextual similarity between two base station IDs $r, q \in \mathcal{R}$ by cosine similarity:

$$\text{sim}_{\text{loc}}(r, q) = \frac{\tilde{\mathbf{x}}_r^\top \tilde{\mathbf{x}}_q}{\|\tilde{\mathbf{x}}_r\|_2 \|\tilde{\mathbf{x}}_q\|_2}. \quad (21)$$

Based on these similarities, we construct a sparse base station graph $G_{\text{loc}} = (\mathcal{R}, E_{\text{loc}})$, where each base station $r \in \mathcal{R}$ is connected to its top- k_{loc} most similar neighbors under $\text{sim}_{\text{loc}}(\cdot, \cdot)$. In our implementation, we set $k_{\text{loc}} = 5$. Formally, the edge set is defined as

$$E_{\text{loc}} = \{(r, q) \mid q \in \mathcal{N}_{k_{\text{loc}}}(r)\}, \quad (22)$$

where $\mathcal{N}_{k_{\text{loc}}}(r)$ denotes the set of top- k_{loc} neighbors of base station r .

Let $\mathcal{C} = \{C_1, C_2, \dots, C_F\}$ be the set of connected components of G_{loc} . Then \mathcal{C} forms a partition of \mathcal{R} :

$$C_i \cap C_j = \emptyset \quad (i \neq j), \quad \bigcup_{f=1}^F C_f = \mathcal{R}. \quad (23)$$

We regard each connected component as a base station category. Accordingly, we define the base station category mapping

$$c: \mathcal{R} \rightarrow \{1, 2, \dots, F\}, \quad (24)$$

where $c(r) = f$ if and only if $r \in C_f$.

Spatial Context Embedding For the current session S , let $\rho \in \mathcal{R}$ denote the base station ID of its last event. We first map ρ to its corresponding category via $c(\rho)$. The spatial context embedding $\mathbf{e}_R^{(\rho)} \in \mathbb{R}^d$ is then defined as

$$\mathbf{e}_R^{(\rho)} = \mathbf{E}_R[c(\rho), :], \quad (25)$$

where $\mathbf{E}_R \in \mathbb{R}^{F \times d}$ is the learnable embedding matrix.

3.4 Cross-Modal Gated Fusion

To effectively integrate heterogeneous yet complementary signals from two distinct modalities, we propose a Cross-Modal Gated Fusion (CMGF) module, as illustrated in Figure 1C, each modality is represented by a feature vector $\mathbf{x}_1, \mathbf{x}_2 \in \mathbb{R}^d$. Unlike typical static fusion schemes, CMGF enables dynamic, content-aware information exchange through a multi-head bilinear interaction mechanism.

Cross-modal interaction For each head $b \in \{1, \dots, B\}$, we first project the input features into query, key, and value subspaces:

$$\begin{aligned} \mathbf{q}_1^{(b)} &= \mathbf{W}_1^{Q(b)} \mathbf{x}_1, & \mathbf{k}_2^{(b)} &= \mathbf{W}_2^{K(b)} \mathbf{x}_2, & \mathbf{v}_2^{(b)} &= \mathbf{W}_2^{V(b)} \mathbf{x}_2, \\ \mathbf{q}_2^{(b)} &= \mathbf{W}_2^{Q(b)} \mathbf{x}_2, & \mathbf{k}_1^{(b)} &= \mathbf{W}_1^{K(b)} \mathbf{x}_1, & \mathbf{v}_1^{(b)} &= \mathbf{W}_1^{V(b)} \mathbf{x}_1, \end{aligned} \quad (26)$$

where $\mathbf{W}_j^{Q(b)}$, $\mathbf{W}_j^{K(b)}$, $\mathbf{W}_j^{V(b)} \in \mathbb{R}^{d_b \times d}$ are learnable projection matrices. The compatibility between modalities is then measured via scaled dot products between cross-modal query-key pairs:

$$\begin{aligned} g_{1 \leftarrow 2}^{(b)} &= \sigma \left(\frac{(\mathbf{q}_1^{(b)})^\top \mathbf{k}_2^{(b)}}{\sqrt{d_k}} \right), \\ g_{2 \leftarrow 1}^{(b)} &= \sigma \left(\frac{(\mathbf{q}_2^{(b)})^\top \mathbf{k}_1^{(b)}}{\sqrt{d_k}} \right), \end{aligned} \quad (27)$$

where $\sigma(\cdot)$ denotes the sigmoid function. These scalar gates $g_{1 \leftarrow 2}^{(b)}, g_{2 \leftarrow 1}^{(b)} \in (0, 1)$ adaptively control how much information should be transferred from one modality to the other.

Gated fusion The gates are applied to the corresponding cross-modal value vectors to obtain modulated features:

$$\mathbf{a}_1^{(b)} = g_{1 \leftarrow 2}^{(b)} \mathbf{v}_2^{(b)}, \quad \mathbf{a}_2^{(b)} = g_{2 \leftarrow 1}^{(b)} \mathbf{v}_1^{(b)}. \quad (28)$$

Finally, the outputs from all B heads are concatenated within each direction and averaged across the two directions to produce the fused representation:

$$\mathbf{z} = \frac{[\mathbf{a}_1^{(1)} \parallel \dots \parallel \mathbf{a}_1^{(B)}] + [\mathbf{a}_2^{(1)} \parallel \dots \parallel \mathbf{a}_2^{(B)}]}{2}. \quad (29)$$

This bidirectional gating and symmetric aggregation ensure that both modalities contribute equitably while preserving multi-granular cross-modal interactions.

3.5 Inter-Session Intent Transition Module

The intention of users during the use of mobile applications is not static and unchanging, but is constantly reshaped over time, context, and recent interactive behavior. Therefore, how to effectively characterize the migration and evolution of user intentions between different sessions is the key in the next app prediction models. This section models dynamic user intent across sessions by fusing integrated session embeddings with short-term immediate signals to capture current decision-making trends. Specifically, we first input the integrated session embedding as a stable long-term intent memory into the Transformer encoder. Subsequently, the immediate intent representation formed by the recent behavior sequence is input into the decoder to capture short-term changes. Finally, the encoder-decoder architecture fuses short-term and long-term user intent to generate dynamic intention embeddings for the next app prediction.

Intent Transition for Encoder: First, we update the comprehensive embedding by incorporating the temporal and spatial-aware embeddings obtained from the CMGF module, as illustrated below:

$$\mathbf{h} = \text{CMGF}(\mathbf{g}, \text{CMGF}(\mathbf{e}_T^{(\tau)}, \mathbf{e}_R^{(\rho)})). \quad (30)$$

CMGF is cross-modal gated fusion module, $\mathbf{h} \in \mathbb{R}^d$. Finally, the comprehensive embedding \mathbf{h} is transformed by an L -layer Transformer Encoder to extract higher-hop structural semantic features. The update for layer ℓ is

$$\begin{aligned} \hat{\mathbf{h}}^{(0)} &= \mathbf{h}, \\ \tilde{\mathbf{h}}^{(\ell)} &= \text{LayerNorm}(\hat{\mathbf{h}}^{(\ell)} + \text{MHSA}(\hat{\mathbf{h}}^{(\ell)})), \\ \hat{\mathbf{h}}^{(\ell+1)} &= \text{LayerNorm}(\tilde{\mathbf{h}}^{(\ell)} + \text{FFN}(\tilde{\mathbf{h}}^{(\ell)})), \end{aligned} \quad (31)$$

where MHSA denotes multi-head self-attention, and FFN is a feed-forward network, $\hat{\mathbf{h}}^{(L)}$ is the final encoded session representation.

Intent Transition for Decoder : To capture the evolution of user preferences, we employ an L -layer Transformer decoder to model intent transitions. Instead of using a static representation, we take the short-term immediate intent s

as the initial query state. The decoding process at layer ℓ is formulated as follows:

$$\begin{aligned}
 \hat{\mathbf{s}}^{(0)} &= \mathbf{s}, \\
 \tilde{\mathbf{s}}_1^{(\ell)} &= \text{LayerNorm}(\hat{\mathbf{s}}^{(\ell)} + \text{MHSA}(\hat{\mathbf{s}}^{(\ell)})), \\
 \tilde{\mathbf{s}}_2^{(\ell)} &= \text{LayerNorm}(\tilde{\mathbf{s}}_1^{(\ell)} + \text{MHA}(\tilde{\mathbf{s}}_1^{(\ell)}, \hat{\mathbf{h}}^{(L)})), \\
 \hat{\mathbf{s}}^{(\ell+1)} &= \text{LayerNorm}(\tilde{\mathbf{s}}_2^{(\ell)} + \text{FFN}(\tilde{\mathbf{s}}_2^{(\ell)})),
 \end{aligned} \tag{32}$$

where MHA denotes multi-head attention, specifically, at layer ℓ , the query is computed from $\tilde{\mathbf{s}}_1^{(\ell)}$, whereas the keys and values are obtained from the encoder’s session representation $\hat{\mathbf{h}}^{(L)}$. The final output of the L -th layer is the representation of session intent Transition $\mathbf{u} = \hat{\mathbf{s}}^{(L)}$.

Next App Prediction: The final representation \mathbf{u} produced by the decoder integrates (1) the structural representation aggregated from multi-hop session graphs, (2) the short-term immediate intent derived from the most recent apps, and (3) contextual information such as temporal and spatial-aware embeddings. \mathbf{u} captures both short-term and long-term behavioral signals as well as external contextual cues, enabling accurate modeling of user preference for the next app. The preference score for app a_i is computed through the dot-product interaction:

$$\begin{aligned}
 \hat{y}_i &= \mathbf{u}^\top \mathbf{e}_A(a_i), \\
 \hat{\mathbf{y}} &= [\hat{y}_1, \hat{y}_2, \hat{y}_3, \dots, \hat{y}_{|\mathcal{A}|}], \\
 \mathbf{P} &= \text{softmax}(\hat{\mathbf{y}}).
 \end{aligned} \tag{33}$$

We obtain the probability $\mathbf{P} = \{\mathbf{P}_1, \mathbf{P}_2, \dots, \mathbf{P}_{|\mathcal{A}|}\}$ of each app by applying the softmax function, the model parameters are learned during training by optimizing the cross-entropy loss:

$$\mathcal{L} = - \sum_{(S, \tau, \rho, a_i) \in \mathcal{T}} y_i \cdot \log \mathbf{P}_i, \tag{34}$$

where \mathcal{T} denotes the training data set. (S, τ, ρ, a_i) indicates that the next app a_i to be launched after the session S (with the temporal context τ and the spatial context ρ), y_i is the ground-truth of the next app.

4 EXPERIMENTS

4.1 Dataset

To evaluate the performance of MISApp, we test MISApp on two real-world datasets: Tsinghua App Usage [42] and LSapp [23], which are widely used for mobile app usage behavior modeling and prediction. Tsinghua App Usage dataset contains additional location information which was fully utilized by our model to predict. The key dataset statistics for these two datasets are summarized in Table 1.

Table 1: Comparison of Tsinghua App Usage and LSapp Datasets

Dataset	Collection Date	Users	Apps	Records	Attributes
Tsinghua App Usage	19–26 April 2016	1000	2000	4, 171, 950	User ID, Timestamp, Base Station ID, App ID, App Category ID, Category Label
LSapp	9 September 2017- 17 May 2018	292	87	3, 658, 590	User ID, Timestamp, Session ID, App ID, Interaction Type

4.2 Experimental Settings

Split Method: During preprocessing, consecutive records of the same app by the same user with an interval of less than 5 minutes were merged to reduce fragmentation. Users with fewer than 50 total app usage events were removed to ensure sufficient data density. Based on the 300 seconds threshold, continuous events were grouped into sessions. Sessions longer than 5000 records were treated as noise and discarded. These steps produce a clean, well-structured dataset suitable for subsequent modeling. For both datasets, we adopt the same cleaning procedures and splitting protocol as used in MAPLE [28].

- **Standard Setting:** For each user, data is divided chronologically into 70% for training, 10% for validation, and 20% for testing. This configuration supports sufficient model learning, parameter tuning, and performance evaluation in a time-aware manner.
- **Cold-Start Setting:** To assess MISApp’s ability to generalize to unseen users, we adopt a user-level split, allocating 90% of users for training and 10% for testing. To ensure a fair comparison, all splits share the same app set, and no new apps are introduced in the test phase.

Evaluation Metrics: To evaluate the effectiveness of the next app prediction, we employ two widely used ranking-based metrics: Accuracy@k (ACC@K) and Mean Reciprocal Rank (MRR@K). Both metrics assess how well the model ranks the true next app among all candidates. ACC@K measures the proportion of test instances where the ground-truth next app appears within the top-k predictions. It is defined as

$$\text{ACC@k} = \frac{1}{N_{test}} \sum_{i=1}^{N_{test}} \mathbb{I}(\text{rank}_i \leq k), \quad (35)$$

where N_{test} represents the test dataset’s total quantity and rank_i is the rank of the i -th correct prediction. MRR@K evaluates how highly the model ranks the correct next app in the predicted list by computing the reciprocal rank:

$$\text{MRR@k} = \frac{1}{N_{test}} \sum_{i=1}^{N_{test}} \frac{1}{\text{rank}_i}. \quad (36)$$

Baselines: We compare MISApp against a comprehensive set of baselines spanning three categories: app usage prediction models, graph-based models, and time-series forecasting architectures.

- **App Usage Prediction Models:** MFU/MRU [21] rely on simple frequency- and recency-based heuristics. AppUsage2Vec [18], DeepApp [26], Appformer [24] and NeuSA [23] employ sequential learning to model contextual app transitions. CoSEM [43] and MAPLE [28] incorporate contextual and semantic embeddings, with MAPLE further leveraging LLM-based representations to enhance prediction.
- **Graph-based Prediction Models:** SA-GCN [32] and Hypergraph-based approaches [34] model relational dependencies among apps through graph or hypergraph structures, enabling higher-order connectivity reasoning in app usage patterns.
- **Time-Series Forecasting Models:** Transformer variants—including Transformer [16], Reformer [36], FEDformer [37], TimesNet [38]—provide strong baselines designed primarily for long-sequence temporal modeling. We additionally include lightweight yet competitive non-Transformer forecasting baselines such as DLinear [44], which adopt linear decomposition strategies for efficient trend–season separation.

DeepApp, DeepPattern and Appformer are evaluated solely on the Tsinghua App Usage dataset, since LSApp does not provide the location data required by these models. On the Tsinghua App Usage dataset, Hypergraph-based model utilize the same graph clustering approach for spatial embedding as employed in our model.

MISApp is configured with an embedding dimension of 64 for app, Temporal Context, and Spatial Context embeddings. The immediate intent window size is set to $K = 3$, and the session length is fixed to $T = 8$. The Transformer encoder consists of 2 layers with 4 attention heads, and the decoder has the same architecture. The Cross-Modal Gated Fusion module employs 4 heads. The LightGCN module is set to $L_g = 2$ propagation layers. Training is performed with a batch size of 512, a learning rate of 0.001, and a dropout rate of 0.10. The model is optimized using the Adam optimizer and trained for 50 epochs.

4.3 Performance Comparison

Results on Standard Setting: As shown in Table 2, MISApp consistently outperforms existing models on both the Tsinghua App Usage and LSApp datasets under the standard evaluation protocol, achieving superior performance across all metrics and demonstrating the effectiveness of its design for the next app prediction in standard settings.

Traditional app usage models such as AppUsage2Vec, DeepApp, DeepPattern, NeuSA, and CoSEM improve over heuristics, yet their reliance on static embeddings or isolated sequence encoders limits their ability to model rich contextual cues. Transformer-based time-series models (Transformer, Reformer, FEDformer, Appformer) further enhance sequence modeling but still implicitly assume homogeneous temporal evolution, often overlooking heterogeneous drivers of app usage such as temporal shifts, cross-app relational patterns. The Hypergraph Model exhibits strong

Table 2: Comparison results under the standard data split. The performance of NeuSA, CoSEM, MAPLE, DeepApp, DeepPattern, and SA-GCN is taken from the MAPLE paper for consistency. The best results are highlighted in bold, and the second-best results are underlined.

Datasets	Tsinghua App Usage					LSapp				
Models	ACC@1	ACC@3	ACC@5	MRR@3	MRR@5	ACC@1	ACC@3	ACC@5	MRR@3	MRR@5
MFU	0.1841	0.3817	0.4881	0.2700	0.2942	0.3025	0.6239	0.7836	0.4418	0.4785
MRU	0.0777	0.2006	0.2615	0.1323	0.1460	0.2001	0.3923	0.5170	0.2792	0.3077
Appusage2Vec	0.3921	0.6447	0.7626	0.5013	0.5289	0.8105	0.9116	0.9416	0.8563	0.8632
Transformer	0.4826	0.6708	0.7342	0.5665	0.5810	0.8173	0.9008	0.9215	0.8554	0.8602
Reformer	0.4803	0.6657	0.7298	0.5629	0.5777	0.8237	0.8937	0.9183	0.8572	0.8620
TimesNet	0.5152	0.7276	0.7971	0.6099	0.6259	0.8374	0.9208	0.9435	0.8754	0.8806
FEDformer	<u>0.5246</u>	<u>0.7372</u>	<u>0.8076</u>	<u>0.6209</u>	<u>0.6364</u>	<u>0.8385</u>	<u>0.9251</u>	<u>0.9464</u>	<u>0.8780</u>	<u>0.8829</u>
DLinear	0.1030	0.1964	0.2612	0.1425	0.1572	0.2461	0.5157	0.6777	0.3588	0.3957
NeuSA	0.4640	0.6562	0.7286	0.5492	0.5658	0.6832	0.8253	0.8830	0.7461	0.7593
SA-GCN	0.0613	0.1882	0.2521	0.1183	0.1331	–	–	–	–	–
DeepApp	0.2862	0.5931	0.7075	0.4210	0.4473	–	–	–	–	–
DeepPattern	0.2848	0.5884	0.7016	0.4185	0.4444	–	–	–	–	–
CoSEM	0.4163	0.6682	0.7499	0.5282	0.5469	0.4990	0.7466	0.8149	0.6083	0.6242
MAPLE	0.5191	<u>0.7385</u>	<u>0.8115</u>	0.6169	0.6338	0.7157	0.8649	0.9150	0.7821	0.7936
Hypergraph Model	0.4790	<u>0.6967</u>	<u>0.7733</u>	0.5761	0.5937	0.8263	0.9111	0.9324	0.8653	0.8702
Appformer	0.2722	0.4770	0.5717	0.2026	0.2015	–	–	–	–	–
MISApp	0.5424	0.7614	0.8277	0.6404	0.6557	0.8394	0.9261	0.9468	0.8790	0.8837

Table 3: Comparison results under the cold-start split. The best results are highlighted in bold, and the second-best results are underlined.

Datasets	Tsinghua App Usage					LSapp				
Models	ACC@1	ACC@3	ACC@5	MRR@3	MRR@5	ACC@1	ACC@3	ACC@5	MRR@3	MRR@5
MFU	0.1840	0.3962	0.5143	0.2759	0.3029	0.2800	0.6433	0.8233	0.4373	0.4786
MRU	0.0000	0.5649	0.6661	0.2637	0.2872	0.0000	0.8549	0.8889	0.4208	0.4287
Appusage2Vec	0.2730	0.4674	0.5757	0.3572	0.3818	0.5354	0.6149	0.6399	0.5698	0.5755
Transformer	0.4877	0.6799	0.7395	0.5740	0.5877	0.7991	0.8965	0.9185	0.8439	0.8489
Reformer	0.4871	0.6764	0.7357	0.5723	0.5859	0.8037	0.8886	0.9118	0.8428	0.8480
TimesNet	0.5159	0.7205	0.7848	0.6074	0.6222	0.8116	<u>0.9095</u>	<u>0.9294</u>	<u>0.8563</u>	<u>0.8609</u>
FEDformer	<u>0.5296</u>	<u>0.7392</u>	<u>0.8024</u>	<u>0.6237</u>	<u>0.6382</u>	<u>0.8126</u>	<u>0.9037</u>	<u>0.9270</u>	<u>0.8542</u>	<u>0.8596</u>
DLinear	0.0795	0.1715	0.2337	0.1191	0.1331	0.3018	0.5229	0.6498	0.4019	0.4303
NeuSA	0.4433	0.6169	0.6812	0.5206	0.5353	0.6874	0.7770	0.8135	0.7272	0.7355
CoSEM	0.3111	0.5597	0.6525	0.4204	0.4416	0.4523	0.7243	0.8104	0.5718	0.5918
MAPLE	0.5228	<u>0.7417</u>	<u>0.8128</u>	<u>0.6206</u>	<u>0.6360</u>	0.7644	0.8848	0.9247	0.8181	0.8272
Hypergraph Model	0.4811	0.6867	0.7553	0.5722	0.5879	0.8088	0.8976	0.9248	0.8491	0.8553
Appformer	0.2813	0.4889	0.5844	0.1820	0.1560	–	–	–	–	–
MISApp	0.5463	0.7614	0.8192	0.6408	0.6544	0.8134	0.9165	0.9350	0.8603	0.8646

performance by modeling higher-order relations, yet standard hypergraphs treat each hyperedge as a set without internal ordering, limiting their capacity to encode sequential transition structures within a session. Moreover, conventional GCN-based architectures may encounter over-smoothing when stacking multiple layers, causing node representations to become indistinguishable. This issue is mitigated in our multi-order graph design, where different hop-level signals are explicitly separated and aggregated without deep neighborhood propagation. MAPLE also achieves excellent results due to leveraging large-scale pretrained representations, though its performance is bounded by substantial parameter size and heavy architectural complexity. In contrast, MISApp combines multi-hop session graphs, lightweight LightGCN attention networks, and dynamic intent modeling form a complementary and efficient design.

Table 4: Ablation Study.

Datasets	Tsinghua App Usage					LSapp				
Models	ACC@1	ACC@3	ACC@5	MRR@3	MRR@5	ACC@1	ACC@3	ACC@5	MRR@3	MRR@5
w/o Multi-hop Graph	0.5300	0.7455	0.8133	0.6264	0.6420	0.8371	0.9062	0.9257	0.8684	0.8729
w/o Temporal Context	0.5311	0.7394	0.8051	0.6242	0.6393	0.8353	0.9124	0.9336	0.8705	0.8754
w/o Spatial Context	0.5301	0.7400	0.8053	0.6239	0.6390	–	–	–	–	–
w/o Decoder	0.4953	0.6885	0.7655	0.5810	0.5986	0.7746	0.9118	0.9384	0.8378	0.8440
MISApp	0.5424	0.7614	0.8227	0.6404	0.6557	0.8394	0.9261	0.9468	0.8790	0.8837

Results on Cold-Start Setting: Under the cold-start evaluation protocol, MISApp also achieves the best performance across all metrics on both datasets (Table 3), with its benefits particularly pronounced when user history is limited. Methods that rely on personalized embeddings or long-term behavioral patterns—such as AppUsage2Vec and other profile-driven baselines—tend to show reduced performance in this setting, as cold-start users lack sufficient historical data to establish stable preference priors. Transformer-style sequence models also show limited effectiveness: by treating app usage as uniformly evolving temporal signals, they struggle to extract reliable intent from extremely short and noisy interaction sequences.

In contrast, MISApp remains highly robust because it does not rely on any user profiles or long-term records. Instead, it reconstructs user intent purely from session-level multi-order structural cues and immediate contextual signals. This design enables MISApp to (i) capture population-level behavioral regularities shared across users, (ii) infer meaningful intent even from minimal interactions, and (iii) maintain strong generalization to completely unseen users. As a result, MISApp consistently demonstrates superior adaptability and resilience in cold-start scenarios.

4.4 Ablation Study

To assess the contribution of each core component, we conduct an ablation study by progressively removing key modules from MISApp. Four variants are evaluated, and the results on the standard split are shown in Table 4.

Without multi-hop graph structure (w/o Multi-hop Graph): This variant removes the multi-hop structural components and retains only the traditional 1-Hop session graph. The performance degradation demonstrates that higher-order structural dependencies contribute meaningful relational signals rather than introducing noise. By explicitly modeling multi-hop transitions, MISApp preserves distinct dependency ranges within the session, which are essential for capturing semantic progression and dynamic intent shifts during app transitions.

Without temporal context (w/o Temporal Context): Removing temporal context embedding deprives MISApp of fine-grained temporal cues that reflect the dynamics of app interactions within a session. The moderate performance drop suggests that while temporal information provides useful contextual signals, the model’s core predictive power primarily stems from structural and intent-aware representations.

Without spatial context (w/o Spatial Context): This variant removes all spatial-aware features, thereby discarding the spatial context necessary to model activity dependent application usage. The more serious performance degradation indicates that the spatial signal has a greater contribution to distinguish the user intention characteristics in Tsinghua App Usage dataset.

Without dynamic intent decoder (w/o Decoder): We disable MISApp’s dynamic intent decoder, relying only on the encoder’s static session representation. This variant suffers the largest performance drop, highlighting that modeling evolving user intent is essential for capturing long-term behavioral dynamics.

4.5 Modal Fusion Study

To evaluate the effectiveness of the Cross-Modal Gated Fusion module, we compare it against several alternative fusion strategies: Sum Fusion, Mean Fusion, CNN Fusion, MLP Fusion and Gated Fusion. The results on the Tsinghua App Usage dataset under the standard split are summarized in Table 5.

Table 5: Performance comparison of different modal fusion strategies.

Methods	ACC@1	ACC@3	ACC@5	MRR@3	MRR@5
Sum	0.5321	0.7429	0.8091	0.6264	0.6416
Mean	0.5340	0.7439	0.8077	0.6284	0.6431
CNN	0.5361	0.7540	0.8212	0.6335	0.6489
MLP	0.5326	0.7395	0.8051	0.6204	0.6391
Gated	0.5382	0.7564	0.8241	0.6358	0.6514
CMGF	0.5463	0.7614	0.8192	0.6408	0.6544

The experimental results show that our method achieves superior performance. Mean Fusion and Sum Fusion directly combine modality representations through element-wise averaging or addition. Although these strategies are simple and computationally efficient, they treat all modalities equally and ignore the varying importance of different modalities, which may lead to suboptimal representations when the contributions of modalities are imbalanced. CNN Fusion first transforms two one-dimensional modality features into a two-dimensional feature representation and then applies

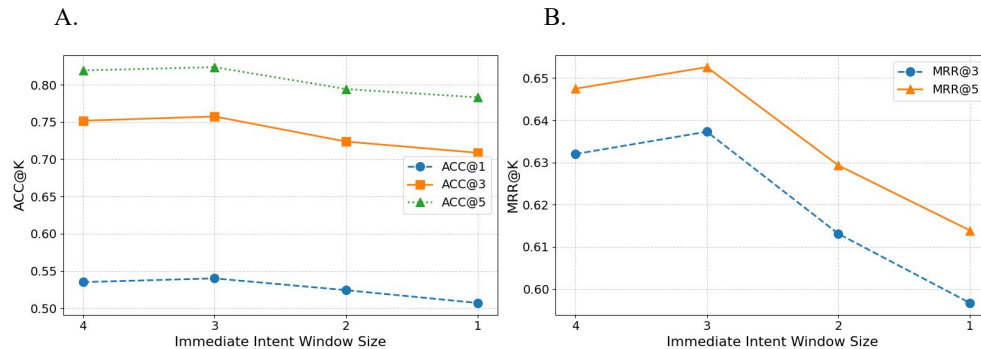


Figure 2: App prediction performance under varying immediate intent window sizes on the Tsinghua App Usage dataset. A. ACC@K evaluation results. B. MRR@K evaluation results.

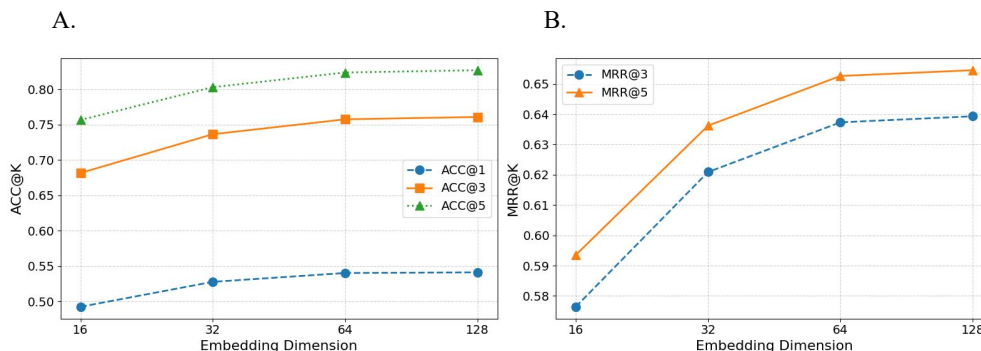


Figure 3: App prediction results with different embedding dimensions on the Tsinghua App Usage dataset. A. ACC@K evaluation results. B. MRR@K evaluation results.

convolution operations to model their interactions, however, convolutional operations focus on local patterns, which may limit their ability to capture global dependencies between modality representations. MLP Fusion concatenates modality features and learns a joint representation through a multilayer perceptron, enabling nonlinear feature interactions. However, it lacks an explicit mechanism to regulate modality importance and may introduce redundant information during the fusion process. Gated Fusion introduces a gating mechanism to dynamically control the contribution of each modality by learning adaptive weights, but the gating scores are usually computed independently and cannot explicitly capture cross-modal interactions. In contrast, the Cross-Modal Gated Fusion explicitly models cross-modal interactions through a gated attention mechanism, enabling the model to adaptively regulate modality contributions while capturing their mutual dependencies, thereby achieving superior performance.

Table 6: Comparison of Practical Efficiency Across App Prediction Methods. Results for MAPLE are taken from their original papers; other results are obtained under the same evaluation setup in our experiments.

Models	Parameters (M)	Model size (MB)	Memory (MB)	Latency Mean (ms)	P95 Latency (ms)	Inference time (s/sample)	ACC@1
DeepApp	2.17	8.29	547	0.6648	0.7348	0.0005e-2	0.2862
DeepPatterns	1.71	6.51	589	0.5054	0.5394	0.0017e-2	0.2848
Appformer	1.48	5.68	1017	286.69	364.39	0.0550e-2	0.2722
Hypergraph Model	1.55	7.95	1006	195.70	200.03	0.0376e-2	0.4790
MAPLE	60.0	480.0	–	–	–	1.1270e-2	0.5191
MISApp	1.32	5.08	435	38.169	43.67	0.0066e-2	0.5424

4.6 Robustness Testing

To further assess the stability and generalization capability of MISApp, we conduct robustness experiments on the Tsinghua App Usage dataset under the standard split by varying several key architectural choices and hyperparameter settings. In particular, we examine how the immediate intent window size, embedding dimension, maximum session window size, and number of Transformer layers affect prediction performance.

Effectiveness of Immediate Intent Window Size: The immediate intent window size controls how many of the most recent app interactions are used to characterize short-term intent. We experiment with $K \in \{1, 2, 3, 4\}$ and observe that small to moderate window sizes consistently improve performance, highlighting the strong predictive value of short-term behavior. As shown in Figure 2, when K becomes excessively large, performance plateaus or slightly declines due to the inclusion of less relevant interactions.

Effectiveness of Embedding Dimension: The overall time complexity of our model is $O(Td(d+T) + d|\mathcal{A}|)$, where T , d , and $|\mathcal{A}|$ denote the session window size, embedding dimension, and number of applications, respectively. Since $T \ll d$ and $T \ll |\mathcal{A}|$, the embedding dimension d becomes the dominant factor affecting both computational overhead and parameter scale. As shown in Figure 3, we evaluate embedding dimensions ranging from 16 to 128, since the performance gain at $d = 128$ is only marginal compared with $d = 64$, we adopt $d = 64$ to achieve a better balance between accuracy and computational efficiency.

Effectiveness of Maximum Session Window Size: We vary the session window size $T \in \{5, 6, 7, 8, 9\}$ to evaluate model stability. As shown in Table 7, moderate session window sizes significantly improve performance by capturing useful historical context, while overly large session windows introduce noise and dilute current preferences. This result further confirms the stability of MISApp and its ability to effectively exploit relevant historical information.

Effectiveness of Transformer Layers: We investigate how the number of Transformer layers affects performance by varying $L \in \{1, 2, 3, 4\}$. Performance improves from $L = 1$ to $L = 2$, whereas deeper architectures lead to diminishing returns or even overfitting. This suggests that a moderately deep architecture with $L = 2$ provides an effective balance between expressive capacity and generalization ability for user intent modeling at the session-level. The experimental results are reported in Table 8.

Table 7: Effect of Maximum Session Window Size W on Model Performance.

T	ACC@1	ACC@3	ACC@5	MRR@3	MRR@5
5	0.5379	0.7509	0.8161	0.6333	0.6483
6	0.5389	0.7540	0.8199	0.6351	0.6503
7	0.5393	0.7556	0.8220	0.6361	0.6514
8	0.5424	0.7614	0.8277	0.6404	0.6557
9	0.5391	0.7571	0.8240	0.6367	0.6521

Table 8: Effect of Transformer Layers L on Model Performance.

L	ACC@1	ACC@3	ACC@5	MRR@3	MRR@5
1	0.5286	0.7369	0.8038	0.6217	0.6317
2	0.5424	0.7614	0.8277	0.6404	0.6557
3	0.5316	0.7417	0.8062	0.6326	0.6404
4	0.5314	0.7415	0.8066	0.6255	0.6405

Table 9: Alignment results for the correlation between hop weights and similarity metrics across sample sequences

Sequence ID	App IDs	Target App ID	sim ₁	sim ₂	sim ₃	W _{hop1}	W _{hop2}	W _{hop3}
Seq-1	[758, 184, 20, 88, 184, 302, 88, 184]	20	1.52	1.52	1.59	0.30	0.33	0.36
Seq-2	[1, 632, 1, 632, 1, 632, 1, 50]	632	3.24	4.50	4.50	0.31	0.34	0.34
Seq-3	[3, 8, 3, 21, 3, 242, 3, 242]	3	1.51	1.30	1.51	0.35	0.30	0.35
Seq-4	[57, 338, 519, 57, 338, 221, 57, 2]	142	0.12	0.12	0.14	0.32	0.33	0.34

4.7 Efficiency and Deployment Analysis

To further evaluate the practicality of existing models for mobile application prediction, we analyze several representative models in terms of their training cost, inference efficiency, and prediction accuracy, as summarized in Table 6. Specifically, we report the number of model parameters, model size, GPU memory consumption during training, inference time per sample, mean inference latency per sample, 95th-percentile inference latency, and Top1 prediction accuracy on the Tsinghua App Usage dataset under the standard split.

Regarding inference efficiency, lightweight baselines such as DeepApp and DeepPatterns achieve low mean inference latency due to their relatively simple architectures. However, their prediction accuracy remains relatively limited. In real-world mobile application prediction scenarios, inaccurate predictions not only degrade user experience through irrelevant recommendations, but also impose additional system-level overhead, therefore, prediction reliability is often more critical than marginal improvements in inference speed.

In contrast, more advanced models such as Appformer, Hypergraph Model, and MAPLE generally provide stronger modeling capability but often introduce higher computational complexity. Compared with these approaches, MISApp achieves the highest prediction accuracy while maintaining a smaller model size and a lower training memory consumption. Although the inference time per sample of MISApp is moderately higher than that of some lightweight baselines, it still remains within an acceptable range for practical online systems.

In general, the results demonstrate that MISApp achieves a better balance between prediction accuracy and computational efficiency, making it suitable for real-world deployment in intelligent mobile service prediction systems where both predictive performance and resource efficiency must be considered.

4.8 Case Study

To demystify the internal reasoning mechanism of MISApp, we investigate whether the learned hop-weights align with the intrinsic structural dependencies of app transitions. Specifically, we conduct two groups of detailed analyses: (1) an alignment study between hop-weights and structural correlations, (2) structured perturbation experiments to assess sensitivity and dependency of critical multi-hop structures.

4.8.1 Alignment of Hop-Weights and Structural Correlation

To verify whether the learned hop-level attention weights (W_{hop_γ}) faithfully capture the intrinsic dependencies within app transition behaviors, we introduce a statistical benchmark based on Pointwise Mutual Information (PMI). Let $\tilde{V}_\gamma^S \subseteq V^S$ denote the set of non-isolated nodes in G_γ^S . Then,

$$sim_\gamma = \frac{1}{|\tilde{V}_\gamma^S|} \sum_{u \in \tilde{V}_\gamma^S} \log \frac{P(u, y)}{P(u)P(y)}. \quad (37)$$

where $P(u, y)$ denotes the joint probability of app u and the target app y co-occurring in a session, and $P(u), P(y)$ represent their respective probabilities of appearing in sessions. All probabilities are estimated from session statistics in the training set.

We first conduct a comprehensive statistical analysis on a critical subset of samples where MISApp successfully predicts the target while the 1-Hop session graph baseline fails. Specifically, we select the 50 samples that exhibit the most significant improvement in prediction probability for the target app when multi-hop structures are introduced. To quantify the alignment between the internal attention of the MISApp and the external transition statistics, we calculate Kendall’s Tau coefficient and the Top-1 Order Consistency Rate. The results show an average Kendall’s coefficient of 0.71 and a Top-1 consistency rate of 0.78, the Kendall’s Tau coefficient data distribution in Table 10, indicating a robust monotonic relationship and a high degree of agreement to identify the most influential hop.

Some sample examples are shown in Table 9. For Seq-1, as illustrated in Figure 4, the applications encompassed by the 3-Hop structure demonstrate stronger semantic relevance and more direct behavioral alignment with the target category (i.e., Entertainment) compared to those captured by the 1-Hop and 2-Hop graphs, as all these applications are directly connected to other apps within the same target category, forming explicit transition links among them. Through multi-hop propagation, the graph effectively filters out incidental or noisy intermediate interactions while preserving transition pathways that reflect consistent user intent. This results in a structural context that is richer in discriminative signals and more closely aligned with the prediction objective, thereby explaining why the 3-Hop graph consistently attracts higher attention weights and plays a more pivotal role in the final prediction.

Table 10: Statistical Distribution of Kendall’s Tau (τ) Correlation.

Correlation Range	Sample Count	Percentage (%)
[0.9, 1.0]	5	10%
[0.8, 0.9)	30	60%
[0.5, 0.8)	7	14%
< 0.5	8	16%

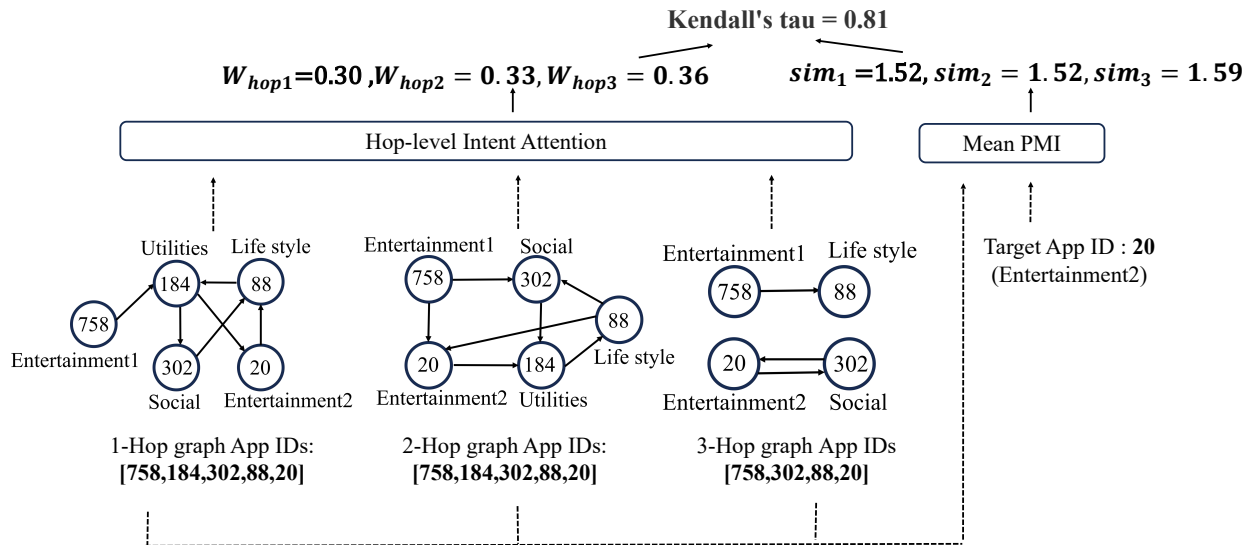


Figure 4: Hop-level weights and structural correlation mechanism for Seq-1. Each app is annotated with both the app ID and its corresponding category label.

4.8.2 Structured Perturbation Experiment

To further evaluate MISApp’s sensitivity to critical structural information in multi-hop session graphs, we design a structured perturbation experiment based on the input sequences presented in Table 9. This experiment investigates whether the model’s predictive probability relies on specific, high-relevance apps within the identified multi-hop session graphs.

- Influential Node Identification:** In the γ -Hop session graph with maximum weight $W_{hop\gamma}$, we identify the most influential app v as the one exhibiting the highest Pointwise Mutual Information (PMI) with respect to the target app y .
- Perturbation Sample Construction:** We generate a perturbed sequence by replacing app v with a noise app v^* , which is selected from a training sequence that exhibits the highest Jaccard similarity to the input sequence, ensuring contextual plausibility while preserving sequential structure.
- Model Inference and Comparison:** The perturbed sequence is fed into the model to recalculate the prediction probability $P(y)$. We compare this with the original probability to assess the model’s ability to capture high-order dependencies.

As observed in Figure 5, under the Top-1 prediction setting, removing high-relevance apps from the maximum weight γ -Hop session graph leads to a substantial drop in the target probability. Based on these sample sequences, when the probability decrease exceeds 0.1, the model fails to maintain its original Top-1 prediction result. This demonstrates that the removed apps carry critical contextual signals for correct inference, and further confirms that our multi-hop reasoning mechanism effectively captures procedural high-order dependencies inherent in user behavior sequences.

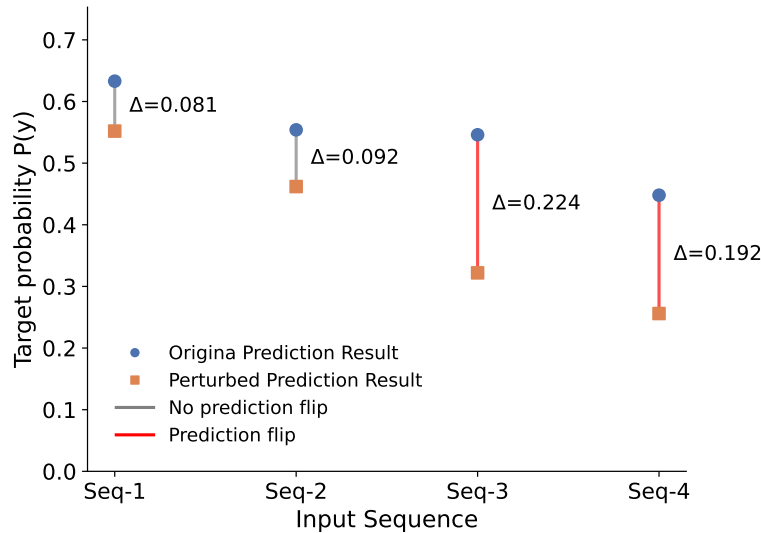


Figure 5: Comparison of Top-1 prediction results and target probabilities under original and perturbed structural settings. Δ denotes the drop in target prediction probability.

5 CONCLUSION

This paper studies next app prediction from the perspective of session-level structural dependency modeling and intent evolution. We show that explicitly modeling multi-hop transition structure provides a more informative view of app usage behavior than conventional sequential or local-transition formulations, especially when user-specific historical information is limited. Built on this idea, MISApp offers a profile-free solution that combines multi-hop session modeling with session-level intent inference. Experimental results on two real-world datasets demonstrate that this design yields strong performance under both standard and cold-start settings, while remaining practically efficient. Moreover, the alignment between learned hop-level attention and structural relevance provides additional support for the interpretability of the proposed framework. Future work will focus on improving efficiency and scalability and on developing lighter variants for deployment in resource-constrained mobile environments.

ACKNOWLEDGMENTS

This work was supported by the National Natural Science Foundation of China under Grant 12471488.

AUTHOR CONTRIBUTIONS

Yunchi Yang: Data curation, Methodology, Software, Validation, Writing—original draft, Writing—review & editing. Longlong Li: Conceptualization, Methodology, Formal analysis, Software, Writing—review & editing. Jianliang Wu: Writing—review & editing. Cunquan Qu: Project administration, Resources, Writing—review & editing.

References

- [1] Tong Li, Mingyang Zhang, Hancheng Cao, Yong Li, Sasu Tarkoma, and Pan Hui. "what apps did you use?": Understanding the long-term evolution of mobile app usage. In *Proceedings of The Web Conference 2020, WWW '20*, page 66–76, New York, NY, USA, 2020. Association for Computing Machinery.
- [2] Yi Ouyang, Bin Guo, Tong Guo, Longbing Cao, and Zhiwen Yu. Modeling and forecasting the popularity evolution of mobile apps: A multivariate hawkes process approach. *Proceedings of the ACM on Interactive, Mobile, Wearable and Ubiquitous Technologies*, 2(4):1–23, 2018.
- [3] Junhong Chu, Haoming Liu, and Alberto Salvo. Air pollution as a determinant of food delivery and related plastic waste. *Nature Human Behaviour*, 5(2):212–220, 2021.

- [4] David J Grüning, Frederik Riedel, and Philipp Lorenz-Spreen. Directing smartphone use through the self-nudge app one sec. *Proceedings of the National Academy of Sciences*, 120(8):e2213114120, 2023.
- [5] Hengshu Zhu, Enhong Chen, Hui Xiong, Huanhuan Cao, and Jilei Tian. Mobile app classification with enriched contextual information. *IEEE Transactions on mobile computing*, 13(7):1550–1563, 2013.
- [6] Yixuan Zhang, Jiaqi Liu, Bin Guo, Zhu Wang, Yunji Liang, and Zhiwen Yu. App popularity prediction by incorporating time-varying hierarchical interactions. *IEEE Transactions on Mobile Computing*, 21(5):1566–1579, 2020.
- [7] Yimin Chen, Xiaocong Jin, Jingchao Sun, Rui Zhang, and Yanchao Zhang. Powerful: Mobile app fingerprinting via power analysis. In *IEEE INFOCOM 2017 - IEEE Conference on Computer Communications*, pages 1–9. IEEE, 2017.
- [8] Adam J. Oliner, Anand P. Iyer, Ion Stoica, Eemil Lagerspetz, and Sasu Tarkoma. Carat: collaborative energy diagnosis for mobile devices. In *Proceedings of the 11th ACM Conference on Embedded Networked Sensor Systems*, SenSys '13, New York, NY, USA, 2013. Association for Computing Machinery.
- [9] Fengli Xu, Yong Li, Huandong Wang, Pengyu Zhang, and Depeng Jin. Understanding mobile traffic patterns of large scale cellular towers in urban environment. *IEEE/ACM transactions on networking*, 25(2):1147–1161, 2016.
- [10] Ming Zeng, Tzu-Heng Lin, Min Chen, Huan Yan, Jiaxin Huang, Jing Wu, and Yong Li. Temporal-spatial mobile application usage understanding and popularity prediction for edge caching. *IEEE Wireless Communications*, 25(3):36–42, 2018.
- [11] Junming Liu, Yanjie Fu, Jingci Ming, Yong Ren, Leilei Sun, and Hui Xiong. Effective and real-time in-app activity analysis in encrypted internet traffic streams. In *Proceedings of the 23rd ACM SIGKDD International Conference on Knowledge Discovery and Data Mining*, KDD '17, page 335–344, New York, NY, USA, 2017. Association for Computing Machinery.
- [12] Yi Ouyang, Bin Guo, Xinjiang Lu, Qi Han, Tong Guo, and Zhiwen Yu. Competitivebike: Competitive analysis and popularity prediction of bike-sharing apps using multi-source data. *IEEE Transactions on Mobile Computing*, 18(8):1760–1773, 2018.
- [13] Tong Li, Tong Xia, Huandong Wang, Zhen Tu, Sasu Tarkoma, Zhu Han, and Pan Hui. Smartphone app usage analysis: Datasets, methods, and applications. *IEEE communications surveys & tutorials*, 24(2):937–966, 2022.
- [14] Enze Lu and Long Zhang. Machine learning methods for smartphone application prediction. In *2022 IEEE 31st International Symposium on Industrial Electronics (ISIE)*, pages 1174–1179, 2022.
- [15] Chengfeng Xu, Pengpeng Zhao, Yanchi Liu, Jiajie Xu, Victor S.Sheng S.Sheng, Zhiming Cui, Xiaofang Zhou, and Hui Xiong. Recurrent convolutional neural network for sequential recommendation. In *The World Wide Web Conference*, WWW '19, page 3398–3404, New York, NY, USA, 2019. Association for Computing Machinery.
- [16] Ashish Vaswani, Noam Shazeer, Niki Parmar, Jakob Uszkoreit, Llion Jones, Aidan N Gomez, Łukasz Kaiser, and Illia Polosukhin. Attention is all you need. In I. Guyon, U. Von Luxburg, S. Bengio, H. Wallach, R. Fergus, S. Vishwanathan, and R. Garnett, editors, *Advances in Neural Information Processing Systems*, volume 30. Curran Associates, Inc., 2017.
- [17] Longlong Li, Cunquan Qu, and Guanghui Wang. Tgt: A temporal gating transformer for smartphone app usage prediction, 2025.
- [18] Sha Zhao, Zhiling Luo, Ziwen Jiang, Haiyan Wang, Feng Xu, Shijian Li, Jianwei Yin, and Gang Pan. Appusage2vec: Modeling smartphone app usage for prediction. In *2019 IEEE 35th International Conference on Data Engineering (ICDE)*, pages 1322–1333. IEEE, 2019.
- [19] Ke Huang, Chunhui Zhang, Xiaoxiao Ma, and Guanling Chen. Predicting mobile application usage using contextual information. In *Proceedings of the 2012 ACM Conference on Ubiquitous Computing*, UbiComp '12, page 1059–1065, New York, NY, USA, 2012. Association for Computing Machinery.
- [20] Xinlei Chen, Yu Wang, Jiayou He, Shijia Pan, Yong Li, and Pei Zhang. Cap: Context-aware app usage prediction with heterogeneous graph embedding. *Proceedings of the ACM on Interactive, Mobile, Wearable and Ubiquitous Technologies*, 3(1):1–25, 2019.
- [21] Choonsung Shin, Jin-Hyuk Hong, and Anind K. Dey. Understanding and prediction of mobile application usage for smart phones. In *Proceedings of the 2012 ACM Conference on Ubiquitous Computing*, UbiComp '12, page 173–182, New York, NY, USA, 2012. Association for Computing Machinery.
- [22] Ricardo Baeza-Yates, Di Jiang, Fabrizio Silvestri, and Beverly Harrison. Predicting the next app that you are going to use. In *Proceedings of the Eighth ACM International Conference on Web Search and Data Mining*, WSDM '15, page 285–294, New York, NY, USA, 2015. Association for Computing Machinery.

- [23] Mohammad Aliannejadi, Hamed Zamani, Fabio Crestani, and W Bruce Croft. Context-aware target apps selection and recommendation for enhancing personal mobile assistants. *ACM Transactions on Information Systems (TOIS)*, 39(3):1–30, 2021.
- [24] Chuike Sun, Junzhou Chen, Yue Zhao, Hao Han, Ruihai Jing, Guang Tan, and Di Wu. Appformer: A novel framework for mobile app usage prediction leveraging progressive multi-modal data fusion and feature extraction. *Expert Systems with Applications*, 265:125903, 2025.
- [25] Jizhe Wang, Pipei Huang, Huan Zhao, Zhibo Zhang, Binqiang Zhao, and Dik Lun Lee. Billion-scale commodity embedding for e-commerce recommendation in alibaba. In *Proceedings of the 24th ACM SIGKDD International Conference on Knowledge Discovery & Data Mining, KDD '18*, page 839–848, New York, NY, USA, 2018. Association for Computing Machinery.
- [26] Tong Xia, Yong Li, Jie Feng, Depeng Jin, Qing Zhang, Hengliang Luo, and Qingmin Liao. Deepapp: Predicting personalized smartphone app usage via context-aware multi-task learning. *ACM Transactions on Intelligent Systems and Technology (TIST)*, 11(6):1–12, 2020.
- [27] Basem Suleiman, Kevin Lu, Hong Wa Chan, and Muhammad Johan Alibasa. Deeppatterns: Predicting mobile apps usage from spatio-temporal and contextual features. In Hakim Hacid, Odej Kao, Massimo Mecella, Naouel Moha, and Hye-young Paik, editors, *Service-Oriented Computing*, pages 811–818, Cham, 2021. Springer International Publishing.
- [28] Yonchanok Khaokaew, Hao Xue, and Flora D Salim. Maple: Mobile app prediction leveraging large language model embeddings. *Proceedings of the ACM on Interactive, Mobile, Wearable and Ubiquitous Technologies*, 8(1):1–25, 2024.
- [29] Aldo Pareja, Giacomo Domeniconi, Jie Chen, Tengfei Ma, Toyotaro Suzumura, Hiroki Kanezashi, Tim Kaler, Tao Schardl, and Charles Leiserson. Evolvegn: Evolving graph convolutional networks for dynamic graphs. *Proceedings of the AAAI Conference on Artificial Intelligence*, 34(04):5363–5370, Apr. 2020.
- [30] Aravind Sankar, Yanhong Wu, Liang Gou, Wei Zhang, and Hao Yang. Dysat: Deep neural representation learning on dynamic graphs via self-attention networks. In *Proceedings of the 13th International Conference on Web Search and Data Mining, WSDM '20*, page 519–527, New York, NY, USA, 2020. Association for Computing Machinery.
- [31] Da Xu, Chuanwei Ruan, Evren Korpeoglu, Sushant Kumar, and Kannan Achan. Inductive representation learning on temporal graphs, 2020.
- [32] Yue Yu, Tong Xia, Huandong Wang, Jie Feng, and Yong Li. Semantic-aware spatio-temporal app usage representation via graph convolutional network. *Proceedings of the ACM on Interactive, Mobile, Wearable and Ubiquitous Technologies*, 4(3):1–24, 2020.
- [33] Yi Ouyang, Bin Guo, Qianru Wang, Yunji Liang, and Zhiwen Yu. Learning dynamic app usage graph for next mobile app recommendation. *IEEE Transactions on mobile Computing*, 22(8):4742–4753, 2022.
- [34] Zihan Huang, Tong Li, Xing Wang, Kexin Yang, Chao Deng, Junlan Feng, and Yong Li. Predicting mobile app usage with context-aware dynamic hypergraphs. *IEEE Transactions on Mobile Computing*, 24(6):5511–5524, 2025.
- [35] Jianling Wang, Kaize Ding, Liangjie Hong, Huan Liu, and James Caverlee. Next-item recommendation with sequential hypergraphs. In *Proceedings of the 43rd International ACM SIGIR Conference on Research and Development in Information Retrieval, SIGIR '20*, page 1101–1110, New York, NY, USA, 2020. Association for Computing Machinery.
- [36] Nikita Kitaev, Łukasz Kaiser, and Anselm Levskaya. Reformer: The efficient transformer, 2020.
- [37] Tian Zhou, Ziqing Ma, Qingsong Wen, Xue Wang, Liang Sun, and Rong Jin. FEDformer: Frequency enhanced decomposed transformer for long-term series forecasting. In Kamalika Chaudhuri, Stefanie Jegelka, Le Song, Csaba Szepesvari, Gang Niu, and Sivan Sabato, editors, *Proceedings of the 39th International Conference on Machine Learning*, volume 162 of *Proceedings of Machine Learning Research*, pages 27268–27286. PMLR, 17–23 Jul 2022.
- [38] Haixu Wu, Tengge Hu, Yong Liu, Hang Zhou, Jianmin Wang, and Mingsheng Long. Timesnet: Temporal 2d-variation modeling for general time series analysis, 2023.
- [39] Xiangnan He, Kuan Deng, Xiang Wang, Yan Li, YongDong Zhang, and Meng Wang. Lightgcn: Simplifying and powering graph convolution network for recommendation. In *Proceedings of the 43rd International ACM SIGIR Conference on Research and Development in Information Retrieval, SIGIR '20*, page 639–648, New York, NY, USA, 2020. Association for Computing Machinery.

- [40] Tong Li, Yong Li, Mingyang Zhang, Sasu Tarkoma, and Pan Hui. You are how you use apps: user profiling based on spatiotemporal app usage behavior. *ACM Transactions on Intelligent Systems and Technology*, 14(4):1–21, 2023.
- [41] Tong Li, Yong Li, Tong Xia, and Pan Hui. Finding spatiotemporal patterns of mobile application usage. *IEEE Transactions on Network Science and Engineering*, pages 1–1, 2021.
- [42] Donghan Yu, Yong Li, Fengli Xu, Pengyu Zhang, and Vassilis Kostakos. Smartphone app usage prediction using points of interest. *Proceedings of the ACM on Interactive, Mobile, Wearable and Ubiquitous Technologies*, 1(4):1–21, 2018.
- [43] Yonchanok Khaokaew, Mohammad Saiedur Rahaman, Ryen W. White, and Flora D. Salim. Cosem: Contextual and semantic embedding for app usage prediction. In *Proceedings of the 30th ACM International Conference on Information & Knowledge Management, CIKM '21*, page 3137–3141, New York, NY, USA, 2021. Association for Computing Machinery.
- [44] Ailing Zeng, Muxi Chen, Lei Zhang, and Qiang Xu. Are transformers effective for time series forecasting? *Proceedings of the AAAI Conference on Artificial Intelligence*, 37(9):11121–11128, Jun. 2023.